

Photocaging of Carboxylic Acids from Cyanine Dyes with Near-Infrared Light**

Hana Janeková, Marina Russo, Urs Ziegler, and Peter Štacko*

Abstract: Near-infrared light (NIR; 650–900 nm) offers unparalleled advantages as a biocompatible stimulus. The development of photocages that operate in this region represents a fundamental challenge due to the low energy of the excitation light. Herein, we repurpose cyanine dyes into photocages that are available on a multigram scale in three steps and efficiently release carboxylic acids in aqueous media upon irradiation with NIR light up to 820 nm. The photocaging process is examined using several techniques, providing evidence that it proceeds via photooxidative pathway. We demonstrate the practical utility in live HeLa cells by delivery and release of the carboxylic acid cargo, that was otherwise not uptaken by cells in its free form. In combination with modularity of the cyanine scaffold, the realization of these accessible photocages will fully unleash the potential of the emerging field of NIR-photoactivation and facilitate its widespread adoption outside the photochemistry community.

Photocages are light-sensitive groups that take advantage of biorthogonality as well as unparalleled spatial and temporal resolution of light as a stimulus to unmask and restore activity of a substrate.^[1] Particularly valued in a biological context, photocages have been used to activate proteins,^[2,3] nucleotides,^[4,5] drugs^[6,7] and other biologically relevant molecules.^[8–10] However, extending their application towards therapeutic utility requires shifting their absorption into the near-infrared (NIR) phototherapeutic window (650–900 nm), a region of wavelengths applicable in the body.^[11,12]

[*] H. Janeková, Dr. M. Russo, Dr. P. Štacko
 Department of Chemistry, University of Zurich
 Winterthurerstrasse 190, 8057 Zurich (Switzerland)
 E-mail: peter.stacko@uzh.ch

Dr. U. Ziegler 0000-0001-7860-1867
 Center for Microscopy and Image Analysis, University of Zurich
 Winterthurerstrasse 190, 8057 Zurich (Switzerland)
 Homepage: 0000-0001-7860-1867

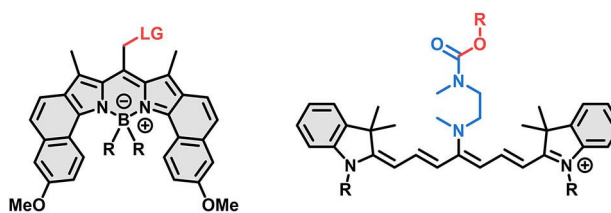
[**] A previous version of this manuscript has been deposited on a preprint server (<https://doi.org/10.26434/chemrxiv-2022-g16fd>).

© 2022 The Authors. Angewandte Chemie International Edition published by Wiley-VCH GmbH. This is an open access article under the terms of the Creative Commons Attribution Non-Commercial NoDerivs License, which permits use and distribution in any medium, provided the original work is properly cited, the use is non-commercial and no modifications or adaptations are made.

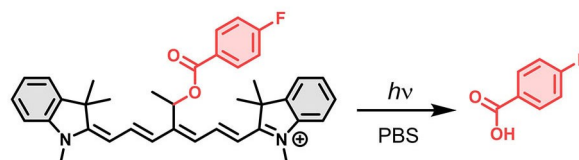
While an impressive collection of organic photocages that can be excited by UV and visible light has been developed in the past decades,^[13] the development of organic, NIR light-activated photocages constitutes a significant challenge in contemporary photochemistry.^[14] Major contributing factors are the low energy of NIR photons, efficient competing deactivation pathways in the excited states and the requirement to operate in aqueous media. Consequently, the entire class of molecules is limited to only few examples (Scheme 1).

Silicon phthalocyanine was shown to release axial phenolic ligands via photoinduced electron transfer in hypoxic conditions.^[15] Schnermann and co-workers harnessed photooxidative cleavage of cyanines (Cy7) to initiate a reaction cascade releasing phenols,^[16–18] but the required linkers preclude release of other groups e.g. carboxylates, amines. Their application in tumor^[19,20] and traumatic brain injury^[21] treatments lends credibility to the use of singlet oxygen-mediated processes in therapeutic settings. Winter and Weinstain independently reported BODIPY photocages with strong green absorption^[22,23] that have since been extensively optimized to improve the photoreleasing efficiencies^[24,25] and extend their absorption maxima towards the edge of the NIR region.^[26] Recently, they were utilized to control oscillations of cardiomyocytes using red light.^[27] Despite significant progress in their design,^[28] BODIPY

State-of-the-art NIR photocages



The concept of this work



Scheme 1. Previously reported NIR-absorbing photocages and the concept of this work. The caged moiety is depicted in red.

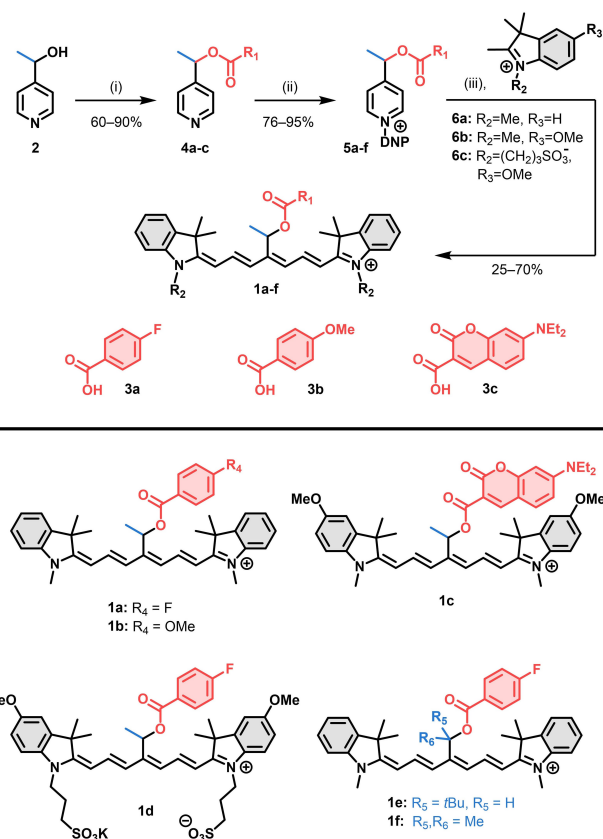
photocages are troubled by lengthy and low yielding synthesis.

On the other hand, theory predicts that analogous release is achievable from Cy3 and Cy7, which share equivalent characteristics of frontier molecular orbitals with BODIPY,^[29,30] leading us to explore this concept. At the time of writing this manuscript, Feringa and co-workers reported similar cyanine-based photocages, suggesting direct photoheterolysis of the C–O bond as the mechanistic pathway of the release.^[31]

Here, we report a heptamethine cyanine-based class of easily accessible photocages that efficiently release carboxylic acids in aqueous media upon irradiation with NIR light up to 820 nm (Scheme 1). We further provide strong experimental evidence that the photouncaging proceeds via photooxygenation pathway instead of direct photoheterolysis. The practical utility of photocages developed in this work is demonstrated by the delivery and release of the carboxylic acid cargo, which is otherwise unable to cross the cell membrane, to live cells using NIR light. A major asset of these photocages is the fact that the caged functionality is attached directly to the cyanine chromophore without additional linkers. Not only does this significantly reduce the complexity of the release process, it also extends the scope of caged functionalities to those previously beyond reach, especially for cyanine photocages (i.e. carboxylates). This particular feature promises high tolerance of our system towards a class of caged moiety that is limited only by the quality of the leaving group.

The photocages were synthesized in 3 steps utilizing our recently developed strategy of ring-opening Zincke salts.^[32] The synthesis started by esterification of carboxylic acids **3a–c** with **2** using EDC.HCl and DMAP in very good to excellent yields (Scheme 2). The pyridines **4a–f** were then transformed to the corresponding Zincke salts **5a–f** by a reaction with 2,4-dinitrophenyl tosylate (DNP) in acetone. Subsequently, **5a–f** were subjected to a one-pot condensation with indolinium-based heterocycles **6a–c** and AcOK to provide the final photocages **1a–f** containing diverse caged carboxylic acids. The methoxy-substituted heterocycle **6c** facilitated preparation of a fully water-soluble derivative **1d**, otherwise inaccessible due to poor reactivity of the *des*-methoxy analogue of **6c**. To demonstrate the practical utility of our protocol, we upscaled the synthesis and successfully prepared ≈ 2 g of the photocage **1a** in a single batch without any detrimental effects on the yield. Attempts to synthesize *des*-methyl analogues of **5a–f** failed and we observed only formation of purple colored, complex mixture of products, presumably due to abstraction of the hydrogen at the methylene position.

UV/Vis absorption spectra of the photocages **1a–f** in PBS (pH 7.4, 10 mM, 20 % DMSO) display intense absorption bands in the NIR region at $\lambda_{\text{abs}} \approx 786\text{--}817$ nm, typical for the heptamethine cyanine dyes (Table 1 and Figure 1A).^[33] It is worth noting that their absorption maxima nearly perfectly match the wavelengths of commercial diode lasers. The compounds **1a–b** also exhibit NIR emission with the Stokes shifts (≈ 23 nm) and quantum yields comparable to that of indocyanine green (ICG). While some derivatives



Scheme 2. Synthesis of the photocages. i) **3a–c**, EDC.HCl, DMAP, CH_2Cl_2 . ii) DNP-OTs, acetone, 40°C . iii) AcOK, EtOH, rt. Caged acids are depicted in red. Counter anions omitted for clarity.

Table 1: Photophysical and photochemical properties of **1a–f**.

	λ_{abs} [nm] ^[a]	λ_{em} [nm] ^[b]	ϵ_{max} [a.c.]	Φ_{F} [%] ^[b]	Φ_{dec} [$\times 10^5$] ^[a,e]
1a	786	809	155 400	2.9 ± 0.7	2.2 ± 0.5
1b	786	808	176 400	3.1 ± 0.1	2.6 ± 0.1
1c	808	844	57 400	$< 2^{[d]}$	46.8 ± 6.6
1d	817	860	123 200	$< 2^{[d]}$	1.7 ± 0.3
1e	796	826	107 100	$< 2^{[d]}$	5.4 ± 0.4
1f	806 ^[b]	843	42 000 ^[b]	$< 2^{[d]}$	$1.3 \pm 0.3^{[b]}$

[a] Determined in PBS. [b] Determined in methanol. [c] The molar absorption coefficient, $\epsilon_{\text{max}}/\text{mol}^{-1} \text{dm}^3 \text{cm}^{-1}$. [d] Values below the detection limit of the setup. [e] Absolute quantum yields of photodecomposition. Average and standard deviations of the mean are given.

displayed propensity to form aggregates at higher concentrations ($> 10^{-5}$ M) in pure PBS buffer, this behavior could be suppressed by the addition of 10 % FBS even at low levels (1 %) of DMSO as a co-solvent (Figure S83–S86). The photocage **1d** did not show significant aggregation behavior even without additional FBS. Nevertheless, the photouncaging studies were carried out with 20 % of DMSO as a co-solvent to facilitate straightforward comparison between all derivatives **1a–f**.

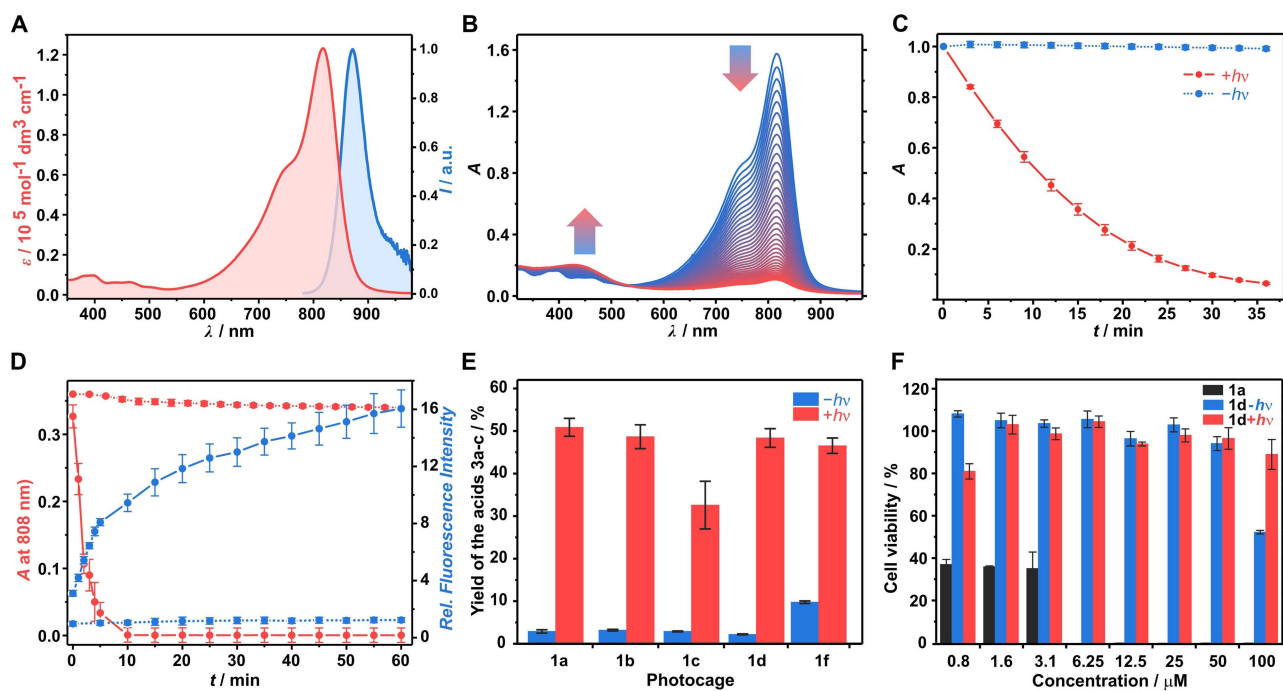


Figure 1. A) Absorption (red) and emission (blue) spectra of **1d** in PBS and methanol, respectively. B) Irradiation of **1b** in PBS at 820 nm followed by UV/Vis spectroscopy every 60 s (blue to red). C) Kinetic trace of the absorption at 817 nm upon irradiation of **1d** at 820 nm (red) and in the dark (blue). D) Absorption (red, $\lambda_{\text{abs}} = 808$ nm) and fluorescence (blue, $\lambda_{\text{exc}} = 390$ nm) traces of **1c** with (solid) or without (dotted) irradiation in PBS at 820 nm. E) Yields of the acids **3a-c** released from **1a-f** upon irradiation (red) and in the dark (blue) determined by HPLC. F) Cell-viability of HeLa cells in the presence of **1a** (black), **1d** (blue) and photoproducts of **1d** (red). Average of three experiments and standard deviations of the mean are given.

The photouncaging ability was initially observed as a build-up of 4-methoxybenzoic acid in ^1H NMR spectra of **1b** left in ambient light over several days (Figure S98). Intrigued by this, we followed irradiation of **1a** in CD_3OD with NIR light at 780 nm (total power ≈ 40 mW) by ^1H and ^{19}F NMR spectroscopies. The irradiation was accompanied by disappearance of the signals of the caged 4-fluorobenzoic acid ($\delta_{\text{F}} \approx -107.1$ ppm) and a concurrent emergence of the signals corresponding to the free acid ($\delta_{\text{F}} \approx -108.7$ ppm; Figure 2A), whereas a sample left in the dark showed no changes, demonstrating that the release is of photochemical origin. The process was found to be complete within 16 h despite high concentration (≈ 3 mM) of **1a**.

We subsequently followed the photouncaging process by UV/Vis absorption spectroscopy. Irradiation of **1a-b**, **1e** ($\lambda_{\text{irr}} \approx 780$ nm; $\approx 50 \text{ mW cm}^{-2}$) or **1c-d** ($\lambda_{\text{irr}} \approx 820$ nm; $\approx 40 \text{ mW cm}^{-2}$) in PBS (pH 7.4, 10 mM, 20% DMSO) was accompanied by depletion of the cyanine absorption band (Figure 1B) and concurrent weak increase of absorption at ≈ 400 nm, attributed to the photobleaching products of the cyanine scaffold.^[34] The photolysis was fully complete within 15–30 min (Figure 1C). The quantum efficiencies of uncaging (Φ_{dec}) are summarized in Table 1 and were found to be comparable to the first generation of BODIPY photocages which, however, operate at wavelengths blue-shifted by > 100 nm.^[26]

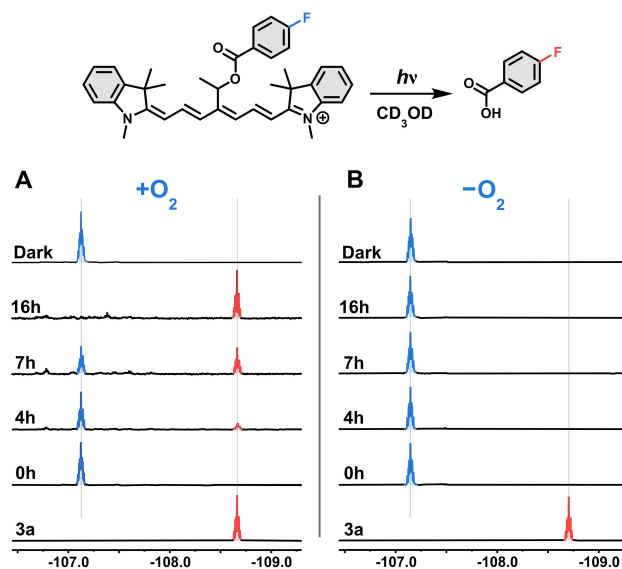


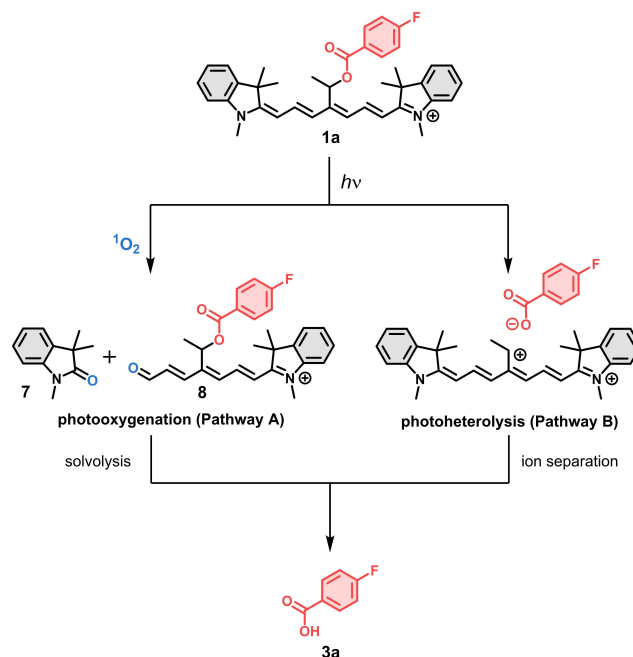
Figure 2. Photouncaging of **3a** upon irradiation at 780 nm followed by ^{19}F NMR spectroscopy in the presence (A) and absence (B) of oxygen.

To follow the photouncaging process in time, we prepared **1c** containing caged fluorescent coumarin-derived acid **3c**, a potent inhibitor of lactate influx in various cancer cell lines.^[35] The coumarin residue in photocage **1c** displays only weak fluorescence signal ($\lambda_{\text{exc}}=420$ nm) due to quenching by energy transfer to the dye. Irradiation of **1c** at 820 nm led to a rapid decrease (within 10 min) of absorption at 808 nm and a simultaneous increase of coumarin fluorescence intensity (≈ 6 -fold) as a consequence of the release of **3c** (Figure 1D; Figure S93). The control samples left in the dark showed no increase of fluorescence intensity.

As the next step, we quantified the chemical yield of carboxylic acids released upon irradiation using HPLC (Figure 1E). The solutions of **1a–f** were irradiated and subsequently incubated at 37 °C for 2 h, whereas the control experiments were incubated in dark at 37 °C for 2 h. The chemical yields of the released carboxylic acids were found to be generally $\approx 50\%$, comparable to the existing NIR photocages.^[16,36] The control experiments incubated in the dark showed only a negligible release ($< 3\%$).

Given the expected biological applications of the photocages, we evaluated the systemic toxicity of **1a** and **1d** on HeLa cells. While photocage **1a** was found to be relatively toxic ($\text{GI} < 5 \mu\text{M}$) in cell viability assays, analogue **1d** with appended solubilizing sulfonate groups and its corresponding photoproducts produced by exhaustive irradiation displayed no toxicity after 24 or 72 h exposure to concentrations as high as 50 μM (Figure 1F and S107). Such distinct effect of the *N*-substituents on the cytotoxicity of cyanine has been previously observed.^[37] Nevertheless, minimal toxicity of **1d** and its photoproducts reinforce the potential of water-soluble analogues of our photocages for applications in biological settings.

We hypothesized two plausible mechanistic explanations for the photouncaging process (Scheme 3)—a self-sensitized photooxidation of the cyanine backbone by singlet oxygen and subsequent dark solvolysis of the photoproducts (Pathway A), or a direct light-initiated heterolysis with concurrent departure of the leaving group (Pathway B). Photooxidation is the primary photobleaching pathway of cyanines that is well documented and proceeds via addition of photogenerated singlet oxygen ($^1\text{O}_2$) on the polyene backbone.^[34] The two pathways can be distinguished by the presence of oxygen. Since Pathway A directly relies on the reactivity of $^1\text{O}_2$, it will be halted in its absence. On the contrary, photoheterolysis B is expected to occur from the triplet excited state,^[24] and its efficacy should therefore increase in the absence of oxygen as the productive excited state is quenched. Our experiments revealed that **1a** is stable to irradiation in degassed CD_3OD (or CD_3OD containing 30 % D_2O) and no release of **3a** was detected by ^1H or ^{19}F NMR spectroscopies (Figure 2B). We also identified ketone **7** as a product of photooxidation^[16,34] of **1a** irradiated under ambient conditions (Figure S99). Analogous photouncaging reactivity was observed when **1a** was irradiated at 590 nm in the presence of methylene blue as an auxiliary singlet oxygen generator (Figure S102, S103). Furthermore, saturating a methanolic solution of **1a** with argon led to ≈ 3 -fold decrease of Φ_{dec} . These observations demonstrate the central



Scheme 3. Plausible mechanisms of the photouncaging process.

role of oxygen in the observed photouncaging and constitute compulsive evidence for the self-sensitized photooxygenation pathway A. This notion is corroborated by the time profile of **3c** uncaging in Figure 1D. The release continued even after the cyanine absorption was fully depleted, suggesting that irradiation is necessary to disrupt the cyanine scaffold and the subsequent step that culminates in the release of the acid occurs in the dark. Treatment of **1a** with an endoperoxide, which thermally generates $^1\text{O}_2$, resulted in analogous release of **3a** in dark (Figure S104, S105), further corroborating the central role $^1\text{O}_2$ in the release mechanism. A potential drawback of the pathway A is the decreased efficiency in hypoxic environments such as solid tumors. The photouncaging proceeds also from **1e** bearing *t*-Bu at the reaction center, suggesting that hydrogens of the methyl group in **1a–d** are not involved in the release.

We reasoned that stabilization of the putative carbocation formed in pathway B could result in favoring the photoheterolysis. Hence, we introduced an additional methyl group at the reaction center in **1f**. The stability of homolog **1f** was compromised, hampering its purification and also manifesting in faster hydrolysis in the dark ($\approx 10\%$ release, Figure 1E). We found that the derivative **1f** was the only photocage that gave rise to a new minor signal ($\delta_{\text{F}} \approx -108.4$ ppm) in the ^{19}F NMR spectra when irradiated with NIR light under oxygen-free conditions (Figure S107–110). This chemical shift, however, did not correspond to that of free acid **3a** ($\delta_{\text{F}} \approx -108.7$ ppm). In addition, HPLC analysis of the mixtures produced by irradiation of **1f** under oxygen-free conditions showed no traces of **3a** and HRMS analysis did not show the presence of a cyanine bearing a methoxy (or hydroxyl group) at the methylene bridge that we

expected to be formed by capturing the putative carbocation with the solvent.

The absence of photouncaging under oxygen-free conditions is in strong contrast with conclusions of the recent report of Feringa and co-workers who, for a photocage related to **1f**, suggested photoheterolysis mechanism (Pathway B) based on indirect evidence using UV/Vis spectroscopy and TD-DFT calculations.^[31] The calculated barrier for the photoheterolytic release in the triplet excited state (T_1) $\Delta G^{\ddagger}_{T1} = 19.0 \text{ kcal mol}^{-1}$ corresponds to the reaction times that are significantly longer (>minutes) than the available T_1 lifetimes of Cy7 (<1 μs).^[38] For instance, related BODIPY photocage derivatives with calculated ΔG^{\ddagger}_{T1} exceeding 15 kcal mol^{-1} failed to release the leaving group upon irradiation^[39] despite T_1 lifetimes comparable to those of Cy7.^[24]

To understand these contradictory results, we synthesized the same photocage bearing acetate cargo^[31] and examined the oxygen dependency of the photouncaging. Irradiation under ambient conditions in d_4 - CD_3OD led to the release of acetate in $\approx 38\%$ yield, whereas in degassed solvent, only a small increase of the release ($\approx 7\%$) compared to the control sample in the dark ($\approx 4\%$) was observed (Figures S113–S116). This minute increase can be ascribed to either integration error, imperfect removal of oxygen or an inefficient photoheterolysis process. Furthermore, the ≈ 150 – 170 -fold discrepancy of quantum yields reported here and in Feringa's work is in excellent agreement with ≈ 150 -fold difference in employed photocage concentrations using different methods of determination. Since only the quantum yield of pathway A should be concentration dependent due the biomolecular reaction between Cy and $^1\text{O}_2$, this notion further supports our mechanism. Therefore, in conjunction with our independent experiments (^{19}F NMR, HPLC, HRMS) conducted under oxygen-free conditions, it can be concluded that the uncaging is, under ambient conditions, dominated by the photooxidation pathway A.

We further tested photouncaging of the fluorogenic coumarin derivative **3c** from **1c** in live cells by fluorescence microscopy experiments. HeLa cells were incubated with **1c** at $37 \pm 1^\circ\text{C}$. The cells were subsequently irradiated at 747 nm with the excitation light source of the microscope. Only very low intensities of both the blue light (390 nm) used for imaging and the red light (747 nm) to trigger uncaging were used to prevent potential phototoxicity. Despite the low quantum yield of free **3c** in aqueous media,^[40] significant increase of the fluorescence intensity in the blue channel (420–450 nm) attributed to the released free **3c** (Figure 3A–C, M) and concomitant depletion of the fluorescence intensity in the red channel (770–850 nm) associated with the photooxidation of the cyanine scaffold **1c** were observed (Figure 3D–F, N). The quantification of the corrected total cellular fluorescence (CTCF) is depicted in Figure 3N–O. The magnitude of the observed relative enhancement in CTCF (≈ 4 – 6 fold) in the blue channel was comparable to that obtained by emission spectroscopy (Figure 1D). In the control studies, only negligible increase in blue fluorescence was observed in the dark (Figure 3G–I),

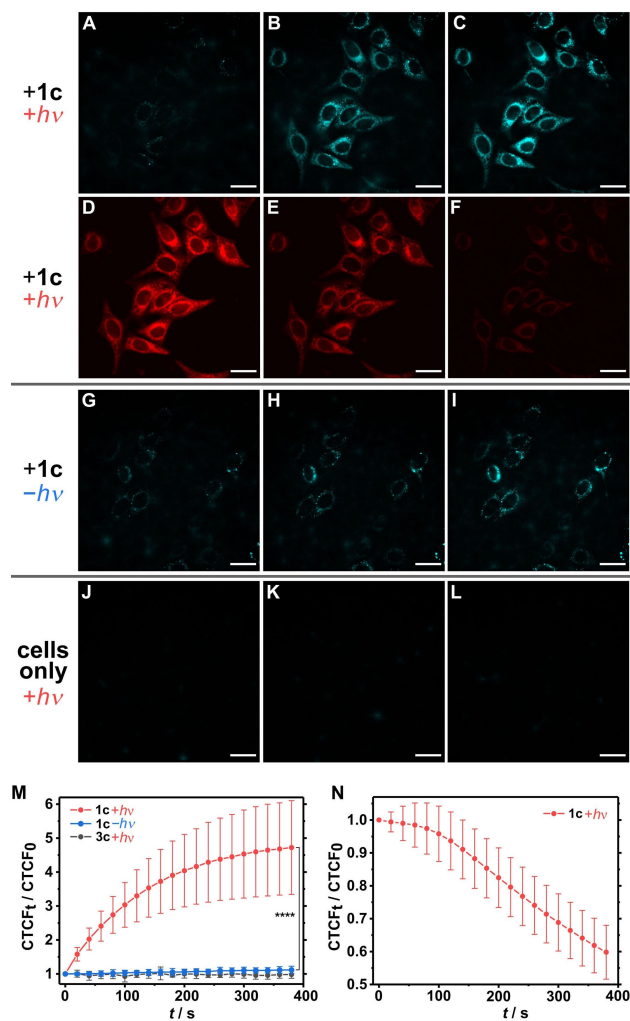


Figure 3. Fluorescence microscopy images of HeLa cells incubated with $3 \mu\text{M}$ of photocage **1c** and irradiated with 747 nm light (cyan coumarin channel A–C; red cyanine channel D–F) or kept in dark (G–I) as a function of time at 0, 140 and 400 s intervals. Irradiation of cells in the absence of **1c** serving as a control experiment (J–L). Plot of CTCF enhancement in HeLa cells in the presence or absence of 747 nm irradiation in the blue (M) and red (N) channels. Average of ≈ 20 – 40 cells and standard deviation of the mean are given. Scale bar represents $30 \mu\text{m}$.

or for cells irradiated in the absence of **1c** (Figure 3J–L). Incubation of HeLa cells with free acid **3c** showed no detectable fluorescence that indicates its poor cellular uptake (Figure S122), presumably due to its anionic nature at physiological pH.^[39] Conjugation of **3c** to a more lipophilic and cationic cyanine scaffold circumvents this issue and facilitates uptake by cells. Our results therefore demonstrate that the photocages can be successfully applied not only for the delivery and release of a cargo with a NIR light trigger in live cells, but also to overcome pharmacokinetic issues of drug-like molecules associated with their poor cellular uptake.

In conclusion, we report a class of photocages that can be synthesized in three steps on multigram scale and release carboxylic acids upon irradiation with NIR light up to 820 nm in aqueous media. The photocaging process was examined independently using ^1H , ^{19}F NMR, emission spectroscopies, and HPLC analysis. The preliminary experiments currently underway in our laboratory suggest that this design is broadly applicable and can be extended towards the release of alcohols and amines. Although the early installation of cargo in these photocages may not be suitable for more complex cargos such as drugs, the efforts to develop a divergent strategy for late-stage introduction of cargos are already underway in our laboratory. In combination with the facile synthesis and modularity of the cyanine scaffold, our readily available photocages constitute an attractive alternative to the existing NIR-uncaging systems. We are convinced that they will make photoactivation using tissue-penetrating light accessible to those non-specialists outside the field of photochemistry, similar to the success of *o*-nitrobenzyl in the past.

Acknowledgements

We gratefully acknowledge Swiss National Science Foundation (SNSF, P.Š/PZ00P2_193425) and the Department of Chemistry, University of Zurich (Legerlotz Stiftung and prof. Hans E. Schmidt Stiftung) for funding of this research project. Imaging was performed with support of the Center for Microscopy and Image Analysis, University of Zurich. We would like to thank Prof. Cristina Nevado, Prof. Karl Gademann and Prof. Michal Juríček (all from University of Zurich) for the generous support of our research. We thank Prof. Jason P. Holland for access to their HPLC, Dr. Katherine Gosselé for assistance with cell-viability assays (both University of Zurich), Nicholas Schilling (University of Zurich) for assistance with microscopy experiments, and Prof. Tomáš Šolomek (University of Bern) and Prof. Petr Klán (Masaryk University) for fruitful suggestions. Open access funding provided by the University of Zurich. Open access funding provided by Universität Zürich.

Conflict of Interest

The authors declare no conflict of interest.

Data Availability Statement

The data that support the findings of this study are available from the corresponding author upon reasonable request.

Keywords: Cyanines · Near-Infrared Light · Photocages · Photooxidation · Photorelease

- [1] P. Klán, T. Šolomek, C. G. Bochet, A. Blanc, R. Givens, M. Rubina, V. Popik, A. Kostikov, J. Wirz, *Chem. Rev.* **2013**, *113*, 119–191.
- [2] D. S. Lawrence, *Curr. Opin. Chem. Biol.* **2005**, *9*, 570–575.
- [3] J. Zhao, J. Zhao, S. Lin, Y. Huang, P. R. Chen, *J. Am. Chem. Soc.* **2013**, *135*, 7410–7413.
- [4] J. H. Kaplan, B. Forbush, J. F. Hoffman, *Biochemistry* **1978**, *17*, 1929–1935.
- [5] J. W. Walker, G. P. Reid, J. A. McCray, D. R. Trentham, *J. Am. Chem. Soc.* **1988**, *110*, 7170–7177.
- [6] Q. Lin, Q. Huang, C. Li, C. Bao, Z. Liu, F. Li, L. Zhu, *J. Am. Chem. Soc.* **2010**, *132*, 10645–10647.
- [7] M. Liu, J. Meng, W. Bao, S. Liu, W. Wei, G. Ma, Z. Tian, *ACS Appl. Bio Mater.* **2019**, *2*, 3068–3076.
- [8] G. Mayer, A. Hechel, *Angew. Chem. Int. Ed.* **2006**, *45*, 4900–4921; *Angew. Chem.* **2006**, *118*, 5020–5042.
- [9] G. C. R. Ellis-Davies, *Nat. Methods* **2007**, *4*, 619–628.
- [10] R. H. Kramer, J. J. Chambers, D. Trauner, *Nat. Chem. Biol.* **2005**, *1*, 360–365.
- [11] R. Weissleder, *Nat. Biotechnol.* **2001**, *19*, 316–317.
- [12] Y. T. Lim, S. Kim, A. Nakayama, N. E. Stott, M. G. Bawendi, J. V. Frangioni, *Mol. Imaging* **2003**, *2*, 50–64.
- [13] R. Weinstain, T. Slanina, D. Kand, P. Klán, *Chem. Rev.* **2020**, *120*, 13135–13272.
- [14] P. Štacko, T. Šolomek, *Chimia Chimia.* **2021**, *75*, 873–881.
- [15] E. D. Anderson, A. P. Gorka, M. J. Schnermann, *Nat. Commun.* **2016**, *7*, 13378.
- [16] A. P. Gorka, R. R. Nani, J. Zhu, S. Mackem, M. J. Schnermann, *J. Am. Chem. Soc.* **2014**, *136*, 14153–14159.
- [17] A. P. Gorka, R. R. Nani, M. J. Schnermann, *Acc. Chem. Res.* **2018**, *51*, 3226–3235.
- [18] T. Yamamoto, D. R. Caldwell, A. Gandioso, M. J. Schnermann, *Photochem. Photobiol.* **2019**, *95*, 951–958.
- [19] R. R. Nani, A. P. Gorka, T. Nagaya, H. Kobayashi, M. J. Schnermann, *Angew. Chem. Int. Ed.* **2015**, *54*, 13635–13638; *Angew. Chem.* **2015**, *127*, 13839–13842.
- [20] R. R. Nani, A. P. Gorka, T. Nagaya, T. Yamamoto, J. Ivanic, H. Kobayashi, M. J. Schnermann, *ACS Cent. Sci.* **2017**, *3*, 329–337.
- [21] C. E. Black, E. Zhou, C. M. DeAngelo, I. Asante, S. G. Louie, N. A. Petasis, M. S. Humayun, *Front. Chem.* **2020**, *8*, 769.
- [22] P. P. Goswami, A. Syed, C. L. Beck, T. R. Albright, K. M. Mahoney, R. Unash, E. A. Smith, A. H. Winter, *J. Am. Chem. Soc.* **2015**, *137*, 3783–3786.
- [23] N. Rubinstein, P. Liu, E. W. Miller, R. Weinstain, *Chem. Commun.* **2015**, *51*, 6369–6372.
- [24] T. Slanina, P. Shrestha, E. Palao, D. Kand, J. A. Peterson, A. S. Dutton, N. Rubinstein, R. Weinstain, A. H. Winter, P. Klán, *J. Am. Chem. Soc.* **2017**, *139*, 15168–15175.
- [25] J. A. Peterson, L. J. Fischer, E. J. Gehrman, P. Shrestha, D. Yuan, C. S. Wijesooriya, E. A. Smith, A. H. Winter, *J. Org. Chem.* **2020**, *85*, 5712–5717.
- [26] J. A. Peterson, C. Wijesooriya, E. J. Gehrman, K. M. Mahoney, P. P. Goswami, T. R. Albright, A. Syed, A. S. Dutton, E. A. Smith, A. H. Winter, *J. Am. Chem. Soc.* **2018**, *140*, 7343–7346.
- [27] K. Sitkowska, M. F. Hoes, M. M. Lerch, L. N. Lameijer, P. Van Der Meer, W. Szymański, B. L. Feringa, *Chem. Commun.* **2020**, *56*, 5480–5483.
- [28] P. Shrestha, K. C. Dissanayake, E. J. Gehrman, C. S. Wijesooriya, A. Mukhopadhyay, E. A. Smith, A. H. Winter, *J. Am. Chem. Soc.* **2020**, *142*, 15505–15512.
- [29] H. E. Zimmerman, S. Somasekhara, *J. Am. Chem. Soc.* **1963**, *85*, 922–927.
- [30] T. Šolomek, J. Wirz, P. Klán, *Acc. Chem. Res.* **2015**, *48*, 3064–3072.

- [31] G. Alachouzos, A. M. Schulte, A. Mondal, W. Szymanski, B. L. Feringa, *Angew. Chem. Int. Ed.* **2022**, *61*, e202201308; *Angew. Chem.* **2022**, *134*, e202201308.
- [32] L. Štacková, P. Štacko, P. Klán, *J. Am. Chem. Soc.* **2019**, *141*, 7155–7162.
- [33] L. Štacková, E. Muchová, M. Russo, P. Slavíček, P. Štacko, P. Klán, *J. Org. Chem.* **2020**, *85*, 9776–9790.
- [34] R. R. Nani, J. A. Kelley, J. Ivanic, M. J. Schnermann, *Chem. Sci.* **2015**, *6*, 6556–6563.
- [35] N. Draoui, O. Schicke, E. Seront, C. Bouzin, P. Sonveaux, O. Riant, O. Feron, *Mol. Cancer Ther.* **2014**, *13*, 1410–1418.
- [36] P. Štacko, L. Muchová, L. Vitek, P. Klán, *Org. Lett.* **2018**, *20*, 4907–4911.
- [37] K. M. Atkinson, J. J. Morsby, S. S. R. Kommidi, B. D. Smith, *Org. Biomol. Chem.* **2021**, *19*, 4100–4106.
- [38] L. Jiao, F. Song, J. Cui, X. Peng, *Chem. Commun.* **2018**, *54*, 9198–9201.
- [39] D. Kand, P. Liu, M. X. Navarro, L. J. Fischer, L. Rousso-Noori, D. Friedmann-Morvinski, A. H. Winter, E. W. Miller, R. Weinstain, *J. Am. Chem. Soc.* **2020**, *142*, 4970–4974.
- [40] A. Chatterjee, D. Seth, *Photochem. Photobiol.* **2013**, *89*, 280–293.

Manuscript received: March 24, 2022

Accepted manuscript online: May 17, 2022

Version of record online: June 1, 2022